PERGAMON

International Journal of Heat and Mass Transfer 42 (1999) 1569–1583

International Journal of HEAT and MASS TRANSFER

Finite element modelling of heat transfer analysis in machining of isotropic materials

M.V. Ramesh[a], K.N. Seetharamu[a,1], N. Ganesan[b,*], G. Kuppuswamy[a]

[a] *Department of Mechanical Engineering, Indian Institute of Technology, Madras 600 036, India*
[b] *Department of Applied Mechanics, Indian Institute of Technology, Madras 600 036, India*

Received 12 March 1997; in final form 7 August 1998

Abstract

A steady state 2-D and 3-D finite element analysis has been carried out for heat transfer analysis in machining of isotropic materials. Using the developed code, reassessment of available literature has been carried out. The effect of the convective heat transfer coefficient in machining has been highlighted. Using empirically available (or experimentally determined) cutting force and feed force values, a numerical model has been developed to predict the tool–chip interface temperature profile.

An extensive parametric study has been carried out for free cutting steels, copper and brass, using cutting data available in the literature, and the results of 3-D analysis are compared with the 2-D analysis and the available literature.

Nomenclature

c_p specific heat at constant pressure
F force
h convective heat transfer coefficient
k thermal conductivity
N shape function
q heat flux
$\dot{Q}$ heat generation rate per unit volume
T temperature distribution in the system
u, v, w velocities
w width of cut or depth of cut.

Greek symbol
ρ mass density.

1. Introduction

It is well known that cutting tool temperature has a critical influence on tool wear and tool life. The rate of cratering is greatly dependent on the tool–chip interface temperature. The growth of crater wear at the tool–chip interface has been found to be directly dependent on the temperature distribution along the interface. In the metal cutting process, the deterioration of the tool is primarily influenced by the stresses induced and the temperature distribution.

A number of experimental techniques have been applied to measure machining temperatures. When machining at normal speeds, temperature gradients are extremely high, especially in the vicinity of the shear plane and the tool–chip interface. Accurate measurement of the temperature distribution is extremely difficult as the chip thickness is very small. Any interference with the machining process such as drilling holes or slots in the chip or tool in an attempt to measure temperatures is likely to alter the temperature distribution. Hence, analytical and numerical methods of solution have been employed to evaluate machining temperatures.

In the tool–chip-work system, temperature distributions along the shear plane and the tool–chip interface are of primary importance. Some of the experimental and analytical investigators have given average values at these regions. The onset of crater wear along the tool rake face is greatly dependent on the magnitude of the maximum temperature. The development of the crater

* Corresponding author
[1] Presently Visiting Professor, School of Mechanical Engineering, Universiti Sains Malaysia, Perak Campus Branch, Tronoh 31750, Malaysia.

0017–9310/98/$ - see front matter
PII: S0017–9310(98)00259–2

has also been shown to correlate highly with the temperature distribution along the interface.

Heat is generated in the primary and secondary zones owing to plastic deformation of the material. Intense heat is also generated along the tool–chip interface due to friction. If the tool is not sharp, some frictional heat will also be generated at the tool–work interface. Most of the heat is carried away by the chip while the rest is conducted through the tool and convected through the work piece due to the movement of the work relative to the cutting edge.

Experimental determination of cutting temperatures has been done by embedded thermocouple, tool–chip thermocouple, radiation pyrometers, thermo color techniques, etc. Arndt and Brown [1] gave an early review on the measurements and the calculation of temperature field for orthogonal machining. Friedman and Lenz [2] have given an analysis of the temperature field in the chip for experimental conditions in the contact zone. Usui et al. [3] have shown that diffusion is the dominant mechanism of cratering in carbide tools. Kato et al. [4] have developed a method for measuring temperature distribution by means of fine powders which have constant melting points. Wright et al. [5] have carried out experiments on low carbon steel tools of different side and rake face geometries. Chow and Wright [6] have obtained the interface temperatures for an interrupted cut and also for a turning operation. Young and Liou [7] have conducted experiments by using an infra-red thermo tracer. In actual practice, it is an arduous task to obtain the temperature distribution in the vicinity of the machining of the materials.

Chao and Trigger [8] have calculated analytically the interfacial temperature distribution by assuming a uniform interfacial heat source. Boothroyd [9] employed semi-analytical methods for obtaining the temperature distributions. Boothroyd's assumption of negligible temperature gradient along the X-direction is not good over significant portions of the chip. He found that a rectangularly distributed heat source appeared to give a better agreement with his experimental results. Venuvinod and Lau [10] have proposed a semi-analytical model for analyzing the temperatures in oblique cutting. By using analytical methods, it is always possible to analyse the maximum tool tip temperatures or temperatures at some locations. It is a difficult task to obtain the temperature distribution. If the material is of anisotropic nature, the difficulty will be many fold.

Rapier [11] has applied a finite difference method to calculate the temperature distribution in machining. He found the temperature gradient perpendicular to the interface to be much lower on the tool side than on the chip side. Dutt and Brewer [12] were the first researchers to consider the work-piece, tool and chip system in solving the energy equation. Along the shear plane, they assumed a uniform plane heat source. Smith and Armarego [13] have used the FDM to calculate a three-dimensional temperature distribution in the tool–chip interface.

Tay et al. [14] were the first to give a finite element model for the temperature distribution. Though a number of investigators have worked on the heat transfer analysis of metal cutting, a good coherence among them has not been found in the literature. The main reasons for this are, the complex geometry, boundary conditions and the lack of proper experimental results for a comparison. Tay [15] has given an excellent review in his recent paper on the methods of calculating machining temperatures. Major among other numerical works are Muraka et al. [16], Smith and Armarego [13], Stevenson et al. [17], Chow and Wright [6], Adil et al. [18], Tay [19].

Tay et al. [14] have calculated machining temperatures by a variational formulation. In this procedure, the flow stress of the work material is a function of strain and strain rate of the shear zone. A simplified version of the procedure was later suggested by Tay et al. [20]. Muraka et al. [16] have developed a finite element model for the temperature distribution in the work-piece, tool and chip during orthogonal machining. This was obtained numerically using the Galerkin approach. The computed results are available for different cutting speeds, feeds, rake angles and tool materials using freshly ground or artificially worn tools with and without coolant. The actual geometries of chip and tool, secondary deformation zones and the variations in density, thermal conductivity and specific heat with temperature have been taken into account. Their analysis is based on the thin shear zone cutting model. Stevenson et al. [17] have compared their finite element results with the temperatures obtained from a metallographic method. This was done for precisely the same tool and work material and close to the same cutting conditions. This procedure has circumvented the need for the flow field as an input. Also, the basic mesh for a given geometry could be automatically adjusted for shear angle and contact length.

Chow and Wright [6] have developed an on-line temperature distribution technique. This has been applied for the case of a turning operation. The tool–chip interface temperature has been estimated by a sensor and is correlated with a finite element model. The measuring scheme obtains the input from a thermocouple, located at the bottom of the tool insert. The scheme could predict the tool–chip interface temperatures for interrupted cutting and also with tool wear. The interface temperatures were used to monitor and control the turning operation.

Adil et al. [18] have presented the temperature analysis of accelerated cutting (taper turning and facing) and also for longitudinal turning using a finite element technique. They have brought out the temperature distribution within the tool–chip-work system and the average tool–chip interface temperature for the two classes of machining viz longitudinal turning and accelerated cutting. Further, they have pointed out that the average tool–

chip interface temperature is lowest in the case of facing. They have shown the temperature distribution by isotherms for taper turning, facing and longitudinal turning. It was observed that the pattern of variation of temperature along the rake face and flank face of the tool are similar during longitudinal turning and facing. The maximum temperature of the rake face and the flank face in all the three cases have been found to occur at some distance away from the cutting edge. The mean tool–chip interface temperature was higher in the case of longitudinal turning and lower for the case of facing as compared to that in taper turning. The average tool–chip interface temperature in all the cases was found to increase with an increase in cutting speed and feed rate.

The existing analytical methods to obtain maximum tool–chip interface temperature, are useful to solve simpler geometries. Where as in a real physical problem it is difficult to get solutions analytically for a complicated system like cutting of a material.

A 3-D model of any manufacturing process represents in more real sense and closed to physics of the problem. It is a very difficult task for any numerical analyst, to perform both pre-processing and post processing of the 3-D analysis. Apart from that, the difficulties faced during computations is manifold when compared to that of a 2-D analysis.

Even though there are several papers related to machining of material, very few researchers have attempted to solve or obtain tool–chip interface temperature profile using 3-D analysis. To obtain a closer insight of machining of materials, a steady state 3-D finite element model has been developed for the heat transfer analysis in the machining. Proper care has been taken to evaluate surface integrals for convective heat transfer boundary conditions.

Ostafiev and Noschchenko [21] have presented a numerical procedure to evaluate the temperature profile in the vicinity of the cutting zone. Using an unsteady state finite element method for heat transfer analysis they have obtained the temperature profile in the cutting zone. However, the effect of convective boundary condition was not clearly brought out.

Lo Casto et al. [22] have employed an FEM to calculate 3-D temperature distributions in the tool alone. They assumed that the temperature at a portion of the tool shank in the tool clamp was constant at the ambient temperature, and a plane uniform frictional heat source existed at the tool–chip contact area. They further assumed that a constant fraction of this frictional heat is conducted into the tool and artificially varied this fraction until the calculated temperature profiles in the tool coincided with that determined experimentally using constant melting point powders.

From the literature, it is observed that even though a number of papers have been published in the prediction of temperatures during machining operation, there are still many uncertainties. They are, the method of imposing the boundary conditions and distribution of heat source. An initial attempt has been made to introduce the heat source obtained from the machining data (either empirical or experimentally obtained) on the primary shear zone.

2. Finite element formulation

2.1. Governing equations and boundary conditions

The heat transfer taking place in tool–chip-work system under steady state in three dimensions is governed by the following partial differential equation

$$k\left(\frac{\partial^2 T}{\partial x^2}+\frac{\partial^2 T}{\partial y^2}+\frac{\partial^2 T}{\partial z^2}\right) -\rho c_{\mathrm{p}}\left(u\frac{\partial T}{\partial x}+v\frac{\partial T}{\partial y}+w\frac{\partial T}{\partial z}\right)+\dot{Q}=0. \quad (1)$$

The boundary conditions applicable are,

(1) $T = T_b$ on part of the boundary Ω_t (2a)

(2) $-k\dfrac{\partial T}{\partial n} = q$ on part of the boundary Ω_q (2b)

(3) $-k\dfrac{\partial T}{\partial n} = h(T-T_\infty)$ on part of the boundary Ω_h. (2c)

Here, n refers to the outward drawn boundary normal to the surface. In the machining process the heat generation is localized. That is why, generally, the heat loss due to radiation is not considered.

The rate of heat generation due to plastic deformation is assumed to be entirely converted into thermal energy in the primary shear deformation zone. Hence, the total energy input to the system is,

$$\dot{Q} = F_{\mathrm{c}}v \quad (3)$$

where Q is the rate of heat generation per unit volume, F_{c} refers to cutting force and v refers to cutting speed.

From metal cutting principles, deducting the frictional energy, $F_{\mathrm{f}}v_{\mathrm{c}}$ from Q, the heat source in the primary deformation zone is given by,

$$\dot{Q} = F_{\mathrm{c}}v - F_{\mathrm{f}}v_{\mathrm{c}}. \quad (4)$$

In the above expression, F_{f} is the feed force and v_{c}, the chip velocity. This heat source is distributed over the primary shear zone.

2.2. Galerkin weighted residual formulation

In the present study a Galerkin weighted residual formulation [16] is employed for the tool–chip-work system. If T represents the approximate temperature solution, then 'R' the residue is given by

$$k\left(\frac{\partial^2 T}{\partial x^2}+\frac{\partial^2 T}{\partial y^2}+\frac{\partial^2 T}{\partial z^2}\right) - \rho c_{\mathrm{p}}\left(u\frac{\partial T}{\partial x}+v\frac{\partial T}{\partial y}+w\frac{\partial T}{\partial z}\right)+\dot{Q}=R \quad (5)$$

where T over the solution domain is equivalent to $[N]\{T_{\mathrm{n}}\}$. $\{T_{\mathrm{n}}\}$ refers to the total nodal temperature vector. $[N]=[N_i, N_j, N_k, \ldots, N_m]$, wherein N_i, N_j, etc., are the shape functions.

These are defined piecewise, element by element and appropriate function for the particular point in space must be used. In the Galerkin weighted residual formulation, the shape function itself is the weighting function. Equating the residue to zero, gives 'n' such equations, which will give in principle, a complete solution for the problem.

After applying the boundary conditions, the governing equation is reduced into 'n' number of simultaneous equations of the form

$$[H]\{T\}=\{F\} \quad (6)$$

in which, H_{ij} and F are given by,

$$H_{ij}=\sum\iiint_e\left(K\frac{\partial N_i}{\partial x}\frac{\partial N_j}{\partial x}\frac{\partial N_k}{\partial x} + K\frac{\partial N_i}{\partial y}\frac{\partial N_j}{\partial y}\frac{\partial N_k}{\partial y}+K\frac{\partial N_i}{\partial z}\frac{\partial N_j}{\partial z}\frac{\partial N_k}{\partial z}\right)\mathrm{d}x\,\mathrm{d}y\,\mathrm{d}z + \sum\iiint_e\left(\rho c_{\mathrm{p}}uN_i\frac{\partial N_i}{\partial x}+\rho c_{\mathrm{p}}vN_i\frac{\partial N_j}{\partial y} + \rho c_{\mathrm{p}}wN_i\frac{\partial N_k}{\partial z}\right)\mathrm{d}x\,\mathrm{d}y\,\mathrm{d}z+\sum\int_{\Omega_h^e}N_ihN_j\,\mathrm{d}\Omega \quad (7)$$

and

$$F_i=\sum\iiint_e N_i\dot{Q}\,\mathrm{d}x\,\mathrm{d}t\,\mathrm{d}z-\sum\int_{\Omega_q^e}N_iq\,\mathrm{d}\Omega+\int_{\Omega_h^e}N_ihT_0\,\mathrm{d}\Omega \quad (8)$$

where Ω_q^e and Ω_h^e refer only to the elements with an external surface on which conditions (2b) and (2c) are specified, respectively. For nodes situated on a boundary of type Ω_T (2a):

$$H_{ij}=\begin{cases}1 & \text{if } i=j\\ 0 & \text{if } i\neq j\end{cases} \quad (9)$$

$$F_i=T_b. \quad (10)$$

Here, $\{T\}$ refers to the column vector containing the nodal temperatures. The $\{T\}$ matrix is obtained by the usual Choleski decomposition.

2.3. Solution methodology

The problem region is divided into eight-noded isoparametric elements. To improve accuracy, the elements are graded in size so that where high temperature gradients are likely to exist, smaller elements are used. The mesh consists of 73 elements with a total of 268 nodes. As different material properties can be specified for each element, it is easy to account for the different thermal properties of both the work piece and tool material as shown in Fig. 1 (front plane). For 3-D analysis, the problem region is divided into eight-noded isoparametric brick elements. The elements are graded in size so that where high temperature gradients are likely to exist, smaller elements are used. As shown in Fig. 1, the mesh consists of 674 elements and 1026 nodes. In z-direction (width of cut) five elements are used. An automatic mesh generation program was developed and used. As different material properties can be specified for each element, it is easy to account for the different thermal properties of both the work piece and tool material.

The element stiffness matrix is assembled into a global stiffness matrix using the direct stiffness procedure and stored in a column vector. After assembling the global stiffness matrix, decomposition into $\mathrm{LDL}^{\mathrm{T}}$ has been carried out. Using back substitution, the solution of the global stiffness matrix is obtained.

3. Results and discussion

The theory presented in Section 2 along with the method of calculation of heat generation is used to predict the temperatures in the tool as this affects tool wear and life. In order to gain confidence in the model developed, comparisons have been carried out wherever adequate data is available in literature.

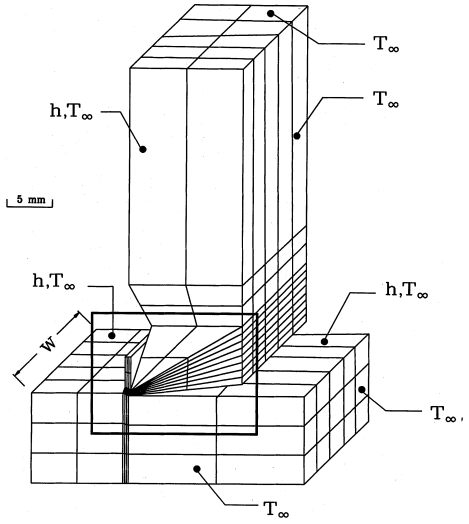

Fig. 1. Details of discretization used—I level.

3.1. 2-D analysis

The results are presented first as verification of the code and some additional data are presented through parametric studies for free cutting steels (both rough and fine cuts), copper and brass materials.

In order to gain confidence in the software developed, an attempt has been made to reproduce the results of Tay et al. [14] for three different speeds. The same geometry and boundary conditions, as used by Tay et al. [14] (Tool consisted of a $12.7 \times 6.35 \times 3.18$ mm tungsten carbide tip brazed to an alloy steel shank $50.8 \times 12.7 \times 12.7$ mm. The tool was clamped on the toolpost by two set screws with an overhang of 11.4 mm. Cutting conditions are: rake angle = 20°, width of cut = 9.50 mm, feed rate = 0.274 mm rev^{-1}, clearance angle = 6° and room temperature $T_\infty = 22$°C and boundary conditions are—convective heat transfer is applied over unmachined, machined, rake face and flank face. Since the heating is localized the rest of the surfaces are imposed with a temperature as ambient.) was considered for the analysis.

Figure 1 (front plane is modeled for 2-D analysis) shows the details of the discretization used in the global sense (I level) consisting of 73 eight-noded isoparametric elements with 268 nodes. Near the tool tip, the size of the elements are of the order of 0.1×0.1 mm as it is necessary to capture the details in that zone. In order to give more details of the mesh, the region enclosed by the rectangle in Fig. 1 is enlarged (zoomed) and is shown in Fig. 2. In order to have a better idea of the mesh near the tool tip, further zooming is carried out as shown in Fig. 3 (for the rectangle portion shown in Fig. 2).

Figure 4 shows the comparison of the predicted temperatures along the rake face for a cutting speed of 29.6 m min^{-1} with that of Tay et al. [14]. As can be observed from Fig. 4, the comparison is good in the sense, the maximum temperature attained (420°C) and the location of the maximum temperature.

Figure 5 shows the comparison of predicted temperatures along the rake face for a cutting speed of 78

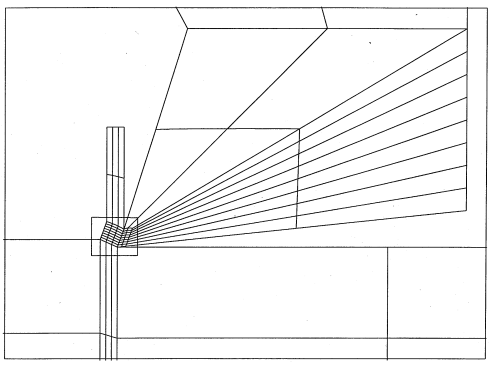

Fig. 2. Details of discretization used—II level.

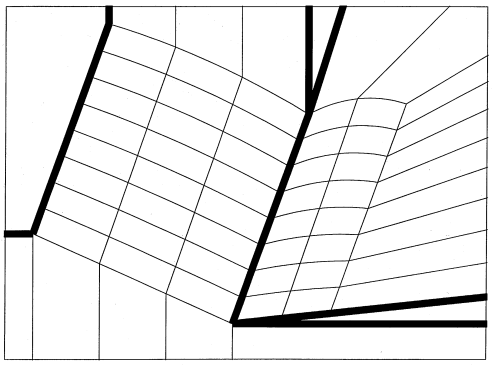

Fig. 3. Details of discretization used—III level.

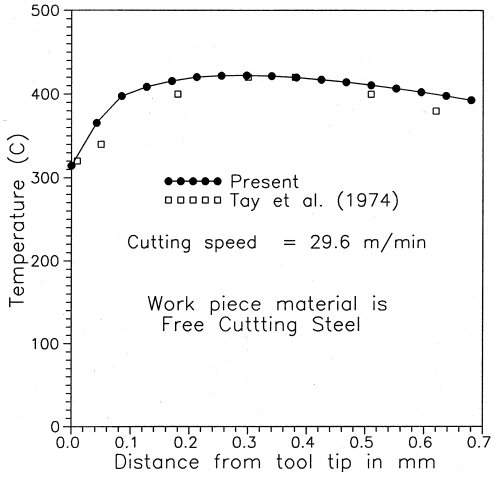

Fig. 4. Comparison of temperatures along the rake face for a cutting speed of 29.6 m min^{-1}.

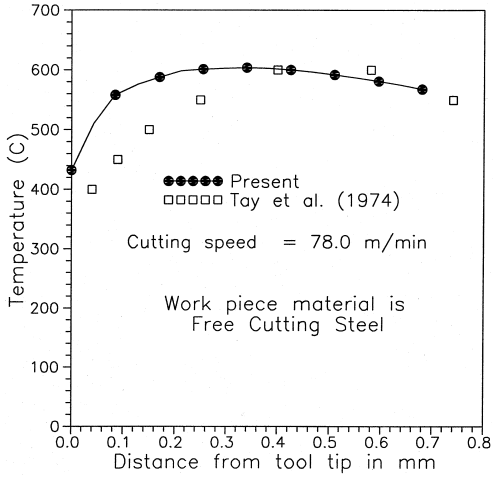

Fig. 5. Comparison of temperatures along the rake face for a cutting speed of 78.0 m min^{-1}.

m min^{-1} with that of Tay et al. [14]. The maximum temperature predicted is the same (600°C). However some difference exists near the tool tip.

Figure 6 shows the comparison for a cutting speed of 155.4 m min^{-1}. It is observed that in Fig. 6 the tool tip temperature is about 440°C, for Tay's case, whereas with the present prediction, it is 680°C, even though the maximum temperature attained in both cases is about 1000°C. The measured temperatures have a profile compared to the present calculated ones as indicated in the reference Usui et al. [3] and Arndt and Brown [1]. Since all the cutting parameters are not available, it is not possible to compare with these research findings. Thus the present prediction is in tune with the measured profiles.

Thus it can be stated, the present model predicts the temperatures reasonably well at the interface region in view of the good comparison with Tay et al. [14].

An attempt has been made to compare the present predictions with that of Muraka et al. [16]. Figure 7 shows the effect of the convective heat transfer coefficient on the several surfaces (including the insulation case where the surface heat transfer coefficient is zero) like tool, chip and work piece. The larger heat transfer coefficient corresponds to the case of effective coolant being used, in which case maximum temperature drastically reduces. Figure 8 shows the comparison of the present data with uniform heat transfer coefficient on all the surfaces and also with a higher heat transfer coefficient on the chip along. It can be observed that the maximum temperature attained is higher than that of Muraka et al. [16] and the trends in present prediction are much higher away from the tool tip. As was pointed out by Tay [15], in his review paper, a temperature of 262°C has been specified by Muraka et al. [16] at the

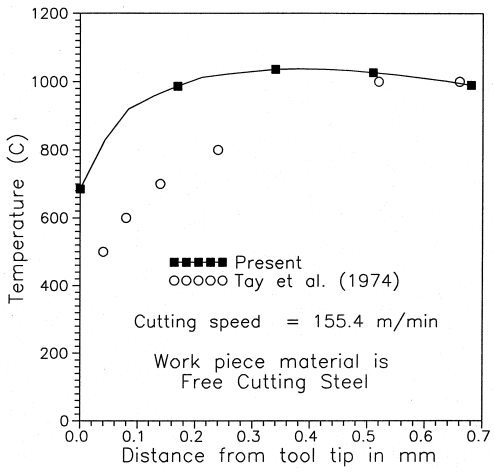

Fig. 6. Comparison of temperatures along the rake face for a cutting speed of 155.4 m min^{-1}.

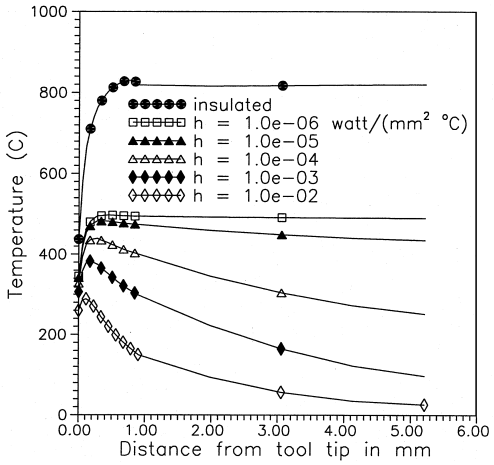

Fig. 7. Effect of heat transfer coefficient on the rake face temperature.

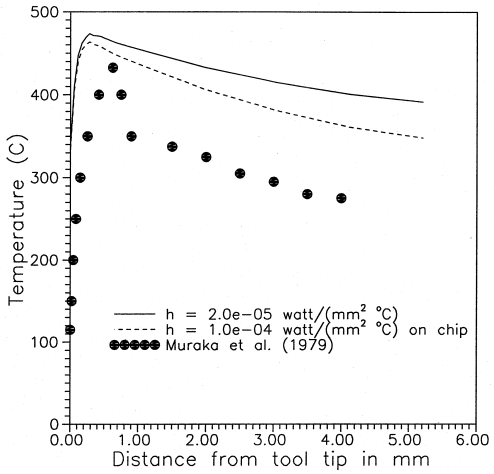

Fig. 8. Effect of different heat transfer coefficients on the chip and tool on rake face temperature.

end of the contact. By specifying the same boundary conditions in the present code, the comparison between the two is reasonably good as shown in Fig. 9. Thus this exercise shows the present code is capable of taking different types of boundary conditions.

In both the above cases, the work piece material used is free cutting steel. In order to gain confidence in the code to apply it to other materials, an attempt has been made to compare the maximum temperature attained in the work piece material, copper, as a function of cutting speed. Figure 10 shows the comparison of predicted maximum tool tip temperatures for the work piece material, copper as a function of cutting speed with the values specified by Trent [23]. There is a reasonably good comparison between the two values and the trend also

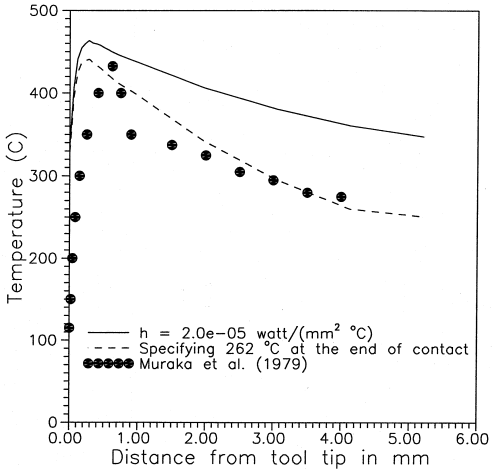

Fig. 9. Comparison of rake face temperature with Muraka et al. [16].

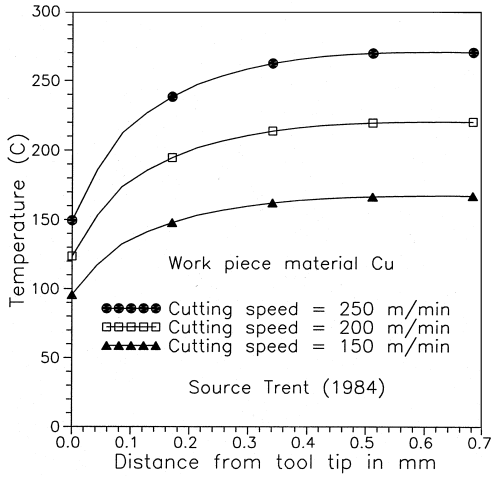

Fig. 11. Effect of cutting speed on rake face temperature for copper.

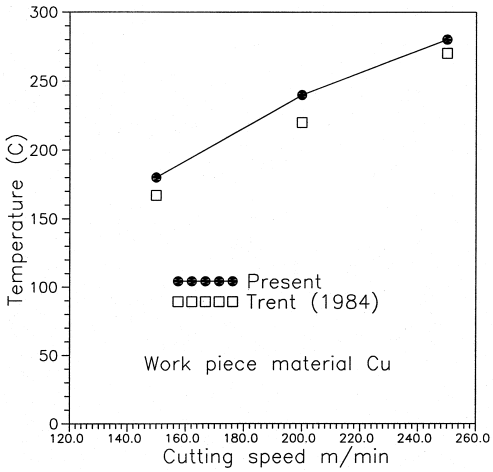

Fig. 10. Comparison of maximum tool tip temperature for copper.

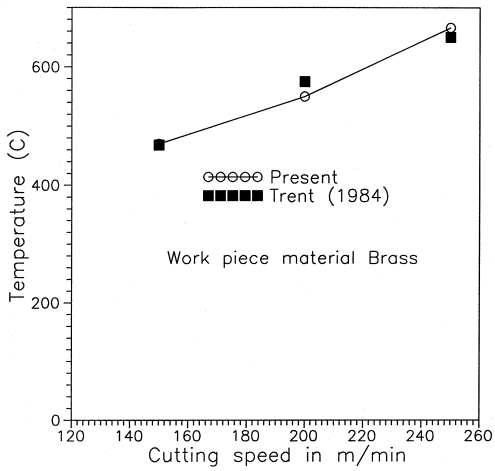

Fig. 12. Comparison of maximum tool tip temperature for brass.

matches very well. Figure 11 shows the effect of cutting speed on the rake face temperatures while machining copper. The cutting data is taken from Trent [23]. It can be seen from Fig. 11, as the speed increases, the temperature increases at a given location. Figure 12 shows similar results to that of Fig. 10 for the work piece material brass. Here again the comparison is good. Figure 13 shows the effect of cutting speed on the rake face temperature for the workpiece material brass and trends are similar to that of Fig. 11.

For practical use, handbooks recommend the cutting conditions to be used for rough and fine machining for various work piece and tool materials. As a typical case, the data presented in the handbook by Kutz [24] for machining free cutting steels is selected for both fine cut and rough cut. This is specifically selected, as the cutting forces can be calculated by empirical formulae [25].

$$F_c = 140.0wf^{0.75}$$

$$F_f = 20.0w^{1.2}f^{0.55} \quad (11)$$

where w is the width of cut in mm and f is the feed rate in mm rev^{-1} and forces are in kgf.

The aim of this exercise is to predict the maximum temperature the tool attains as it influences the tool wear and life. The effect of several parameters on the rake face temperature has also been studied. Figure 14 shows the effect of depth of cut on rake face temperature for fine cuts in free cutting steel. It can be observed that the maximum temperature occurs away from the tool tip as expected. As the depth of cut increases, the temperature decreases at a given location. However, the effect of depth

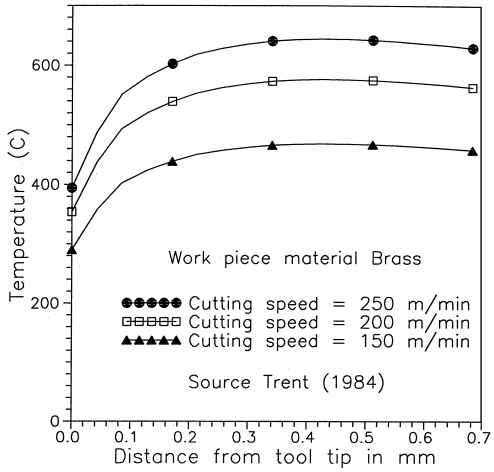

Fig. 13. Effect of cutting speed on rake face temperature for brass.

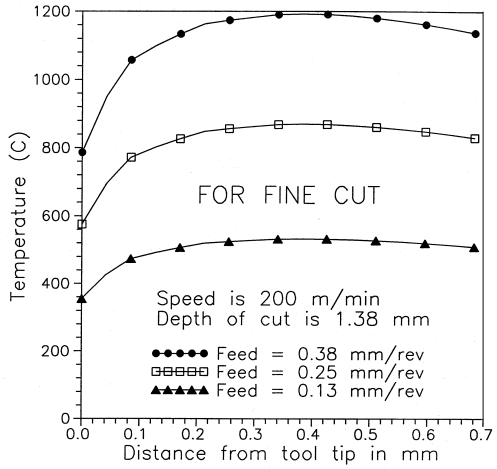

Fig. 15. Effect of feed on rake face temperature for fine cut of free cutting steel.

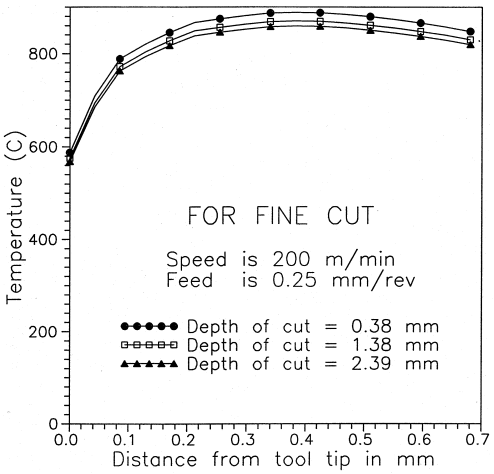

Fig. 14. Effect of depths of cut on rake face temperature for fine cut of free cutting steel.

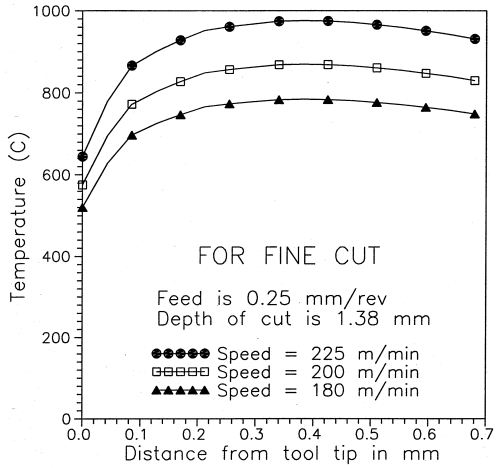

Fig. 16. Effect of speed on rake face temperature for fine cut of free cutting steel.

of cut on temperature is not predominant. Figure 15 shows the effect of feed on the rake face temperature for fine cuts in free cutting steels. As expected, the maximum temperatures are attained away from the tool tip. The effect of feed on the temperatures is quite significant. Figure 16 shows the effect of speed on rake face temperature. The temperature at a given location increases with speed as expected. Figure 17 shows the effect of depth of cut on the rake face temperature for rough cutting of free cutting steels. The maximum temperature occurs away from the tool tip as expected. However, the effect of depth of cut on temperature is marginal for rough cutting. The maximum temperatures attained for rough cut is more than that of fine cut as both depth of cut and feed are much higher for rough cut compared to fine cut. Figure 18 shows the effect of feed on the rake face temperature for rough cutting of free cutting steels.

Speed has substantial effect on the rake face temperature. Figure 19 shows the effect of the speed on rake face temperature for a rough cut on free cutting steels. The trends observed in Fig. 16 is repeated in this case. Figures 20 and 21 show the isotherms in the cutting tool near the tool tip region. As can be observed from both the figures, the maximum temperature occurs away from the tool tip as observed by many investigators.

3.2. 3-D analysis

The ultimate aim of any thermal analysis of machining is a 3-D analysis taking into account the work piece, chip

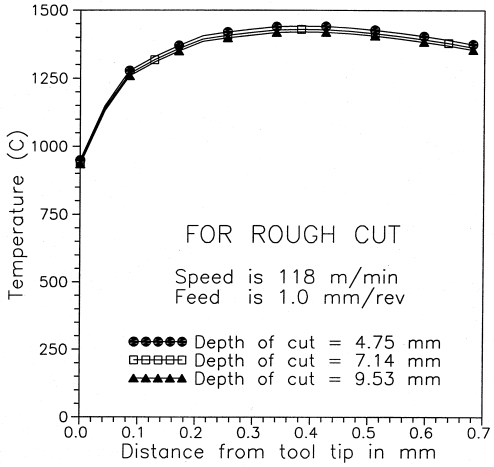

Fig. 17. Effect of depths of cut on rake face temperature for rough cut of free cutting steel.

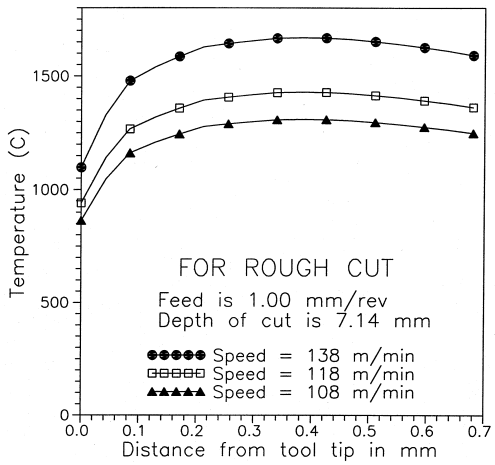

Fig. 19. Effect of speed on rake face temperature for rough cut of free cutting steel.

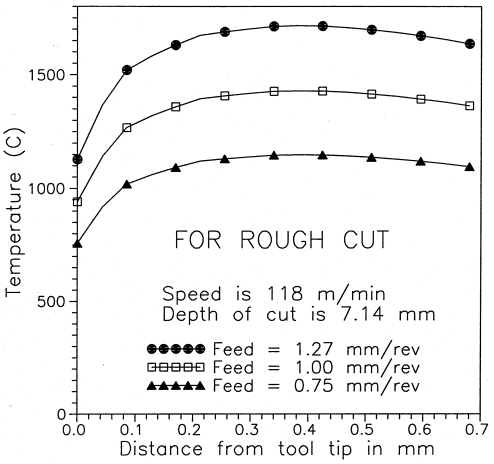

Fig. 18. Effect of feed on rake face temperature for rough cut of free cutting steel.

and the tool. An attempt has been made to develop a 3-D model. The primary objective in developing a 3-D code is to see how much deviation is likely to occur from the 2-D case.

Since the number of papers concerned with 3-D analysis of the machining process is limited and also complete details of any paper are not available, a simple problem with various boundary conditions is considered to validate the program. The problem was so chosen as to provide symmetry in the solution which can be checked. Figure 22(a) shows a cube with a fixed temperature of 100°C on the center line and a fixed temperature of 20°C on four edges. The solution shows symmetry as expected. In Fig. 22(b), the center line temperature is replaced by a heat source. The solution indicates the symmetry as expected. In both the above cases all surfaces are insulated. In Fig. 22(c) the first problem is modified with convective boundary conditions on left- and right-hand-side faces. The symmetry conditions are clearly seen in the solution. The effect of convective heat transfer coefficients are clearly brought out. Figure 22(d) shows the modification to the case (a) by providing constant and equal fluxes on the two side faces. The solution clearly shows the symmetry, thus the program has been tested under various conditions. In the 3-D analysis, eight-noded isoparametric brick elements were used.

The 2-D problems presented in an earlier sub-section corresponding to Tay et al. [14] for three cutting speeds was reconsidered. The discretization of the work piece, chip and tool (width of cut was taken in z-direction while discretizing the tool, chip and work piece) was carried out using 674 eight-noded isoparametric brick elements with 1026 nodes. Figure 23 shows the comparison of rake face temperatures between 2-D and 3-D along with the prediction of Tay et al. [14] for a speed of 29.6 m min^{-1}. It can be observed from Fig. 23 that temperature levels are lower in the case of 3-D compared to 2-D as expected in view of heat conduction in the transverse direction. The maximum temperature attained is about 390°C. The temperature profile along the rake face predicted by 3-D follows the experimental trends as indicated by Usui et al. [3] and Arndt and Brown [1]. Figure 24 shows the comparison for a speed of 78 m min^{-1}. The temperatures predicted from 3-D analysis are lower compared to 2-D. The maximum temperature attained is around 585°C. Figure 25 shows the comparison for a speed of 155.4 m min^{-1}. The temperatures are slightly lower than that of 2-D. However, one important point to be observed is that the tool tip temperatures follow the present predictions from 2-D analysis rather than that of Tay et al. [14] especially in the case of 78.0 m min^{-1} and 155.4 m min^{-1}.

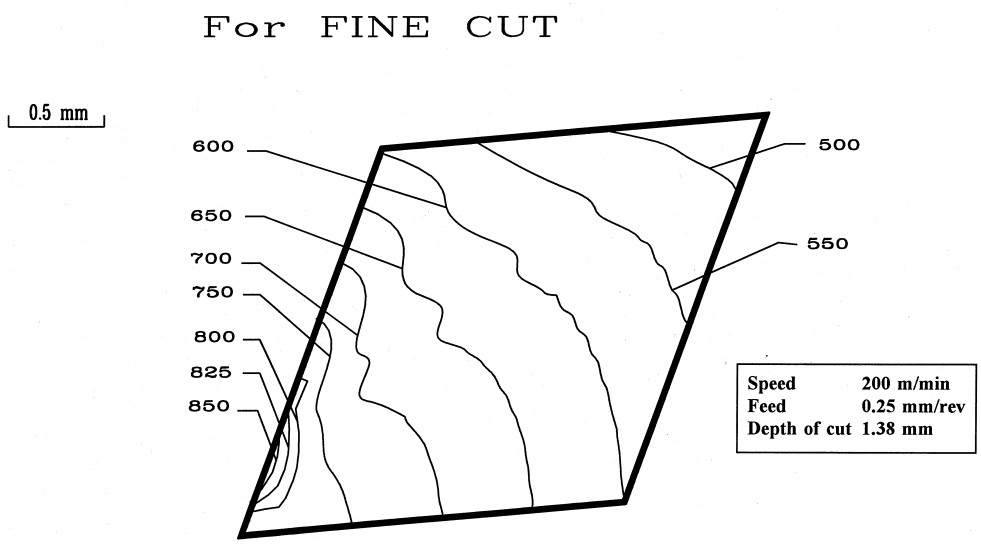

Fig. 20. Temperature distribution in the tool near the tip for fine cut of free cutting steel.

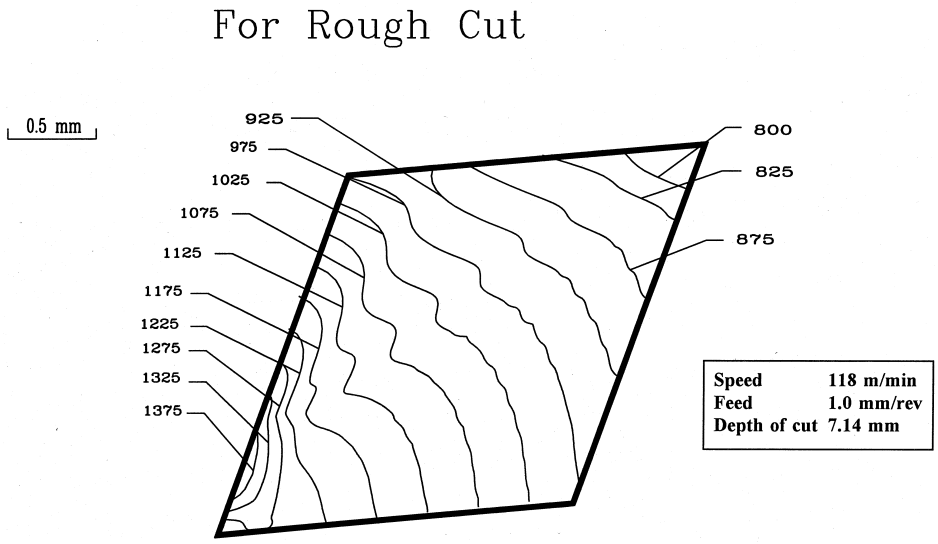

Fig. 21. Temperature distribution in the tool near the tip for rough cut of free cutting steel.

Figure 26 shows the effect of cutting speed on maximum temperature for machining of the work piece material, copper. The results of the 2-D and 3-D analysis are shown along with that of Trent [23]. It can be observed that the predictions from 3-D analysis are less compared to 2-D analysis as expected. The 3-D analysis gives predictions which are slightly lower than that of Trent [23], whereas, the predictions from 2-D are slightly higher than that of Trent [23]. It can be observed from Fig. 27 that the predicted temperatures are lower as expected than that of 2-D analysis. The more important aspect is the predicted temperature profiles for all the three speeds follow the trends of the experimental trends as indicated in Usui et al. [3] and Arndt and Brown [1]. Figure 28 shows the comparison of maximum tool temperature between 2-D and 3-D analysis along with that of Trent [23] for machining brass. The 3-D predictions are generally lower than the 2-D predictions and the comparison is good. Figure 29 shows the effect of cutting speed on the rake face temperature for machining brass based materials based on 3-D analysis. The comments made for Fig. 27 also holds good for Fig. 29.

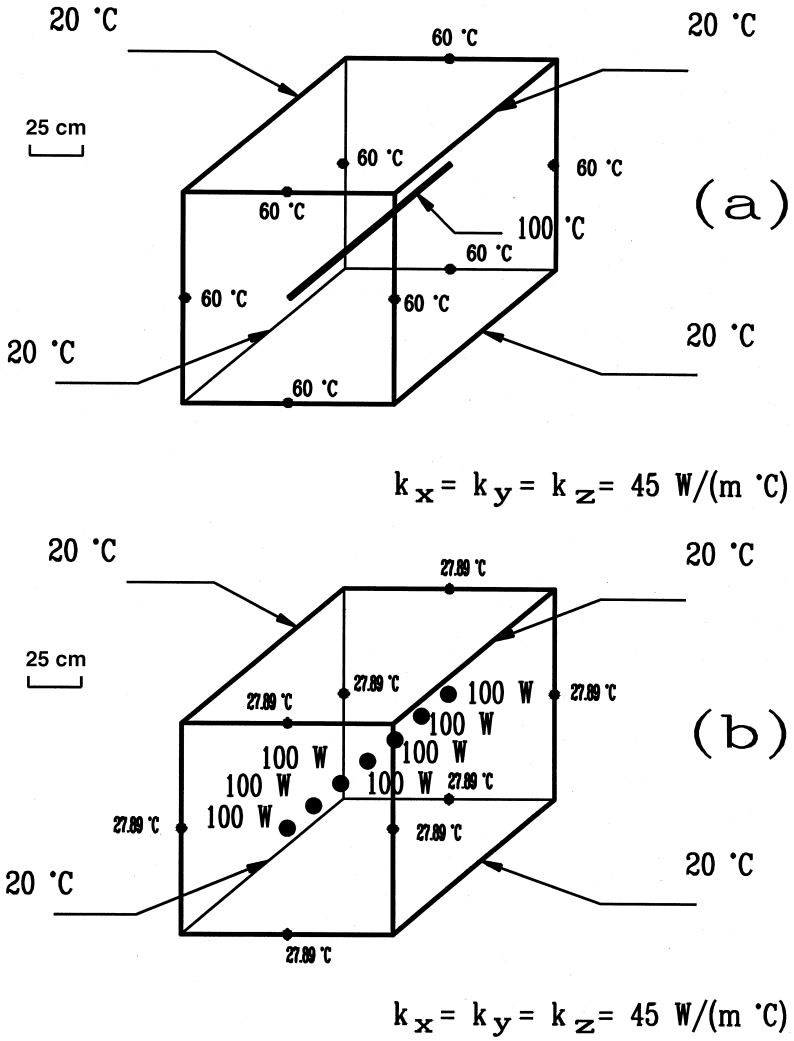

Fig. 22. Verification of the 3-D code.

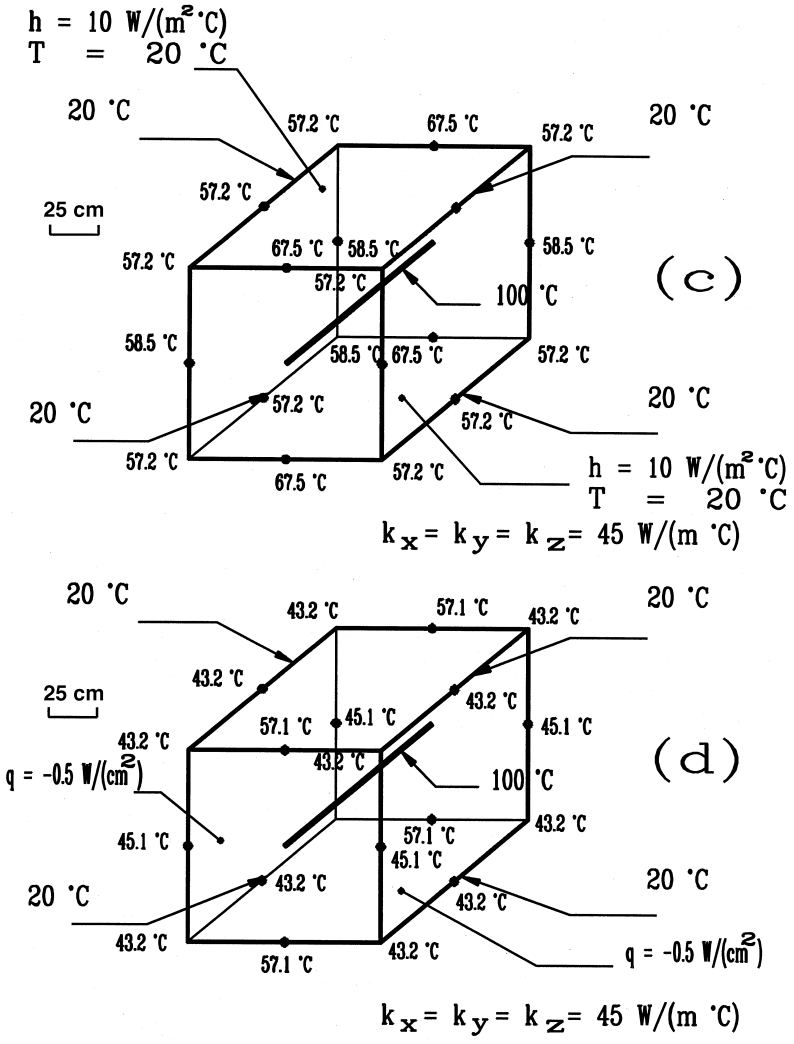

Fig. 22 (*continued*)

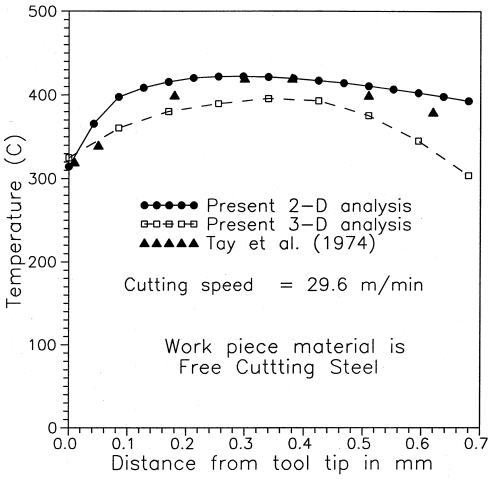

Fig. 23. Comparison of rake face temperature between 2-D and 3-D analysis along with Tay et al. [14] for a speed of 29.6 m min^{-1}.

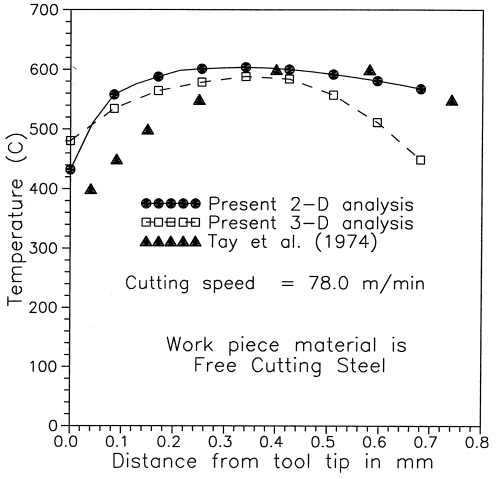

Fig. 24. Comparison of rake face temperature between 2-D and 3-D analysis along with Tay et al. [14] for a speed of 78.0 m min^{-1}.

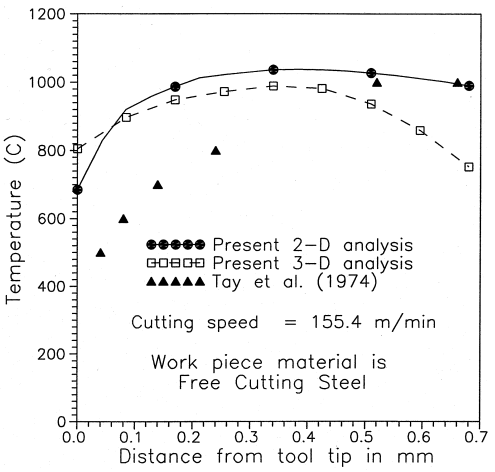

Fig. 25. Comparison of rake face temperature between 2-D and 3-D analysis along with Tay et al. [14] for a speed of 155.4 m min^{-1}.

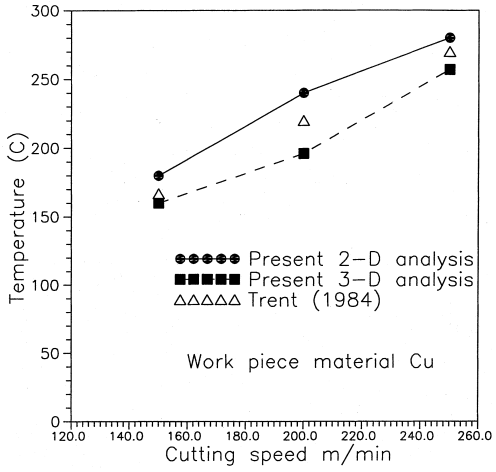

Fig. 26. Effect of cutting speed on maximum temperature—comparison of 2-D and 3-D analysis along with that of Trent [23] for copper.

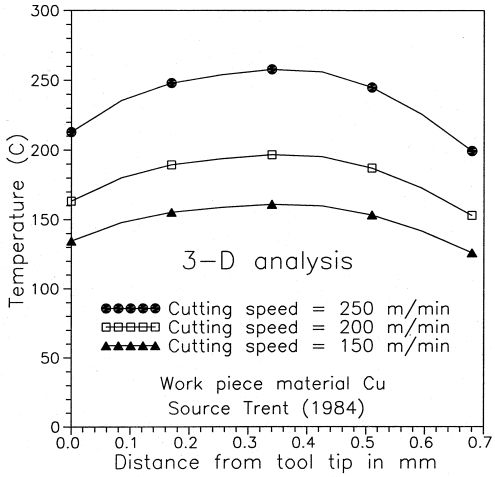

Fig. 27. Effect of cutting speed on the rake face temperature for copper—3-D analysis.

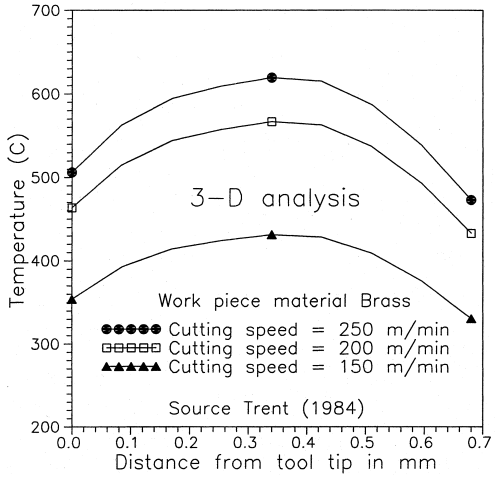

Fig. 29. Effect of cutting speed on the rake face temperature for brass—3-D analysis.

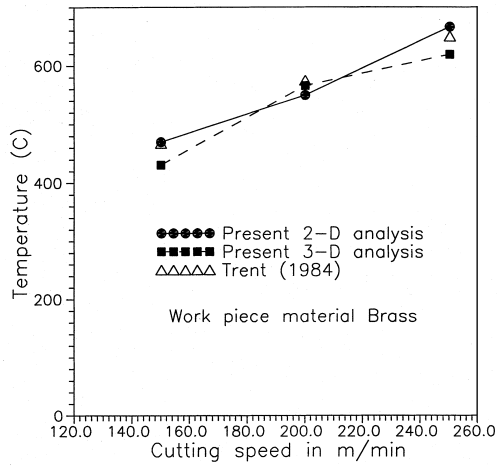

Fig. 28. Comparison of maximum tool temperature between 2-D and 3-D analysis with that of Trent [23] for brass.

4. Conclusions

Both the 2-D and 3-D models of finite element method have been applied for heat transfer analysis in machining of isotropic materials. After observing carefully these conclusions are observed.

- The predictions from the 2-D analysis compare well with those available in the literature.
- The effect of depth of cut on rake face temperature is only marginal.
- The effects of feed and speed on temperatures are significant.
- The predicted temperatures are slightly lower from 2-D analysis because of heat conduction in the third direction.
- The trends of predicted temperature profiles using 3-D analysis follow more closely the experimental trends.
- The effect of depth of cut on rake face temperature is only marginal.
- The effects of feed and speed on temperatures are significant.

References

[1] G. Arndt, R.H. Brown, On the temperature distribution in orthogonal machining, International Journal of Machine Tools Manufacture Design Research and Applications 7 (1967) 39–53.

[2] M.Y. Friedman, E. Lenz, Analysis of temperature field in chip, Journal of Engineering for Industry, Transactions of ASME 95 (1973) 317–320.

[3] E. Usui, T. Shirkashi, T. Kitagawa, Analytical prediction of three dimensional cutting processes, Journal of Engineering for Industry, Transactions of ASME 100 (1978) 236–243.

[4] S. Kato, K. Yamaguchi, Y. Watanabe, Y. Hiraiwa, Measurement of temperature distribution within tool using powders of constant melting point, Journal of Engineering for Industry, Transactions of ASME 98 (1976) 607–613.

[5] P.K. Wright, S.P. McCormick, T.R. Miller, Effect of rake face design on cutting tool temperature distributions, Journal of Engineering for Industry, Transactions of ASME 102 (1980) 123–128.

[6] J.G. Chow, P.K. Wright, On-line estimation of tool/chip interface temperatures for a turning operation, Journal of Engineering for Industry, Transactions of ASME 110 (1988) 56–64.

[7] H.T. Young, Y. Liou, On the analysis of chip temperature distribution in orthogonal cutting, International Journal of

Machine Tools Manufacture Design Research and Applications 34 (1994) 73–84.
[8] B.T. Chao, K.J. Trigger, Temperature distribution at the tool–chip interface in metal cutting, Journal of Engineering for Industry, Transactions of ASME 77 (1955) 1074–1121.
[9] G. Boothroyd, Temperatures in orthogonal metal cutting, Proceedings of Institution of Mechanical Engineers 177 (1963) 789.
[10] P.K. Venuvinod, W.S. Lau, Estimation of rake temperatures in free oblique cutting, International Journal of Machine Tools Manufacture Design Research and Applications 26 (1986) 1–14.
[11] A.C. Rapier, A theoretical investigation of the temperature distribution in the metal cutting process, British Journal of Applied Physics 5 (1954) 400–405.
[12] R.P. Dutt, R.C. Brewer, On the theoretical determination of the temperature field in orthogonal machining, International Journal of Production Research 4 (1964) 91–114.
[13] A.J.R. Smith, E.J.A. Armarego, Temperature prediction in orthogonal cutting with a finite difference approach, Annals of the CIRP 30 (1981) 9–13.
[14] A.A.O. Tay, M.G. Stevenson, G. Vahl Davis, Using the finite element method to determine temperature distributions in orthogonal cutting, Proceedings of Institute of Mechanical Engineers 188 (1974) 627–638.
[15] A.A.O. Tay, A review of methods of calculating machining temperature, Journal of Materials Processing Technology 36 (1993) 225–257.
[16] P.D. Muraka, G. Barrow, S. Hinduja, Influence of the process variables on the temperature distribution in orthogonal machining using the finite element method, International Journal of Mechanical Sciences 21 (1979) 445–456.
[17] M.G. Stevenson, P.K. Wright, J.G. Chow, Further developments in applying the finite element method to the calculation of temperature distributions in machining and comparisons with experiment. Journal of Engineering for Industry, Transactions of ASME 105 (1983) 149–154.
[18] G.K. Adil, V.K. Jain, T. Sundararajan, A finite element analysis of temperature in accelerated cutting, International Journal of Machine Tools Manufacture Design Research and Applications 28 (1988) 577–591.
[19] A.A.O. Tay, The importance of allowing for the variation of thermal properties in the numerical simulation of temperature distribution in machining, Journal of Material Processing and Technology 28 (1991) 49–58.
[20] A.A.O. Tay, M.G. Stevenson, G. vahl Davis, P.L.B. Oxley, A numerical method for calculating temperature distributions in machining, from force and shear angle measurements, International Journal of Machine Tools Manufacture Design Research and Applications 16 (1976) 335–349.
[21] Ostafiev, A.N. Noshchenko, Numerical analysis of three-dimensional heat exchange in oblique cutting, Annals of the CIRP 34 (1985) 137–140.
[22] S. Lo Casto, E. Lo Valvo, F. Micari, Measurement of temperature distribution within tool in metal cutting: experimental tests and numerical analysis, Proceedings of 2nd International CIRP Conference on New Manufacturing Technology, Cookeville, June 1989, pp. 35–46.
[23] E.M. Trent, Metal Cutting, Butterworths, London, 1984.
[24] Myer Kutz (Ed.), Mechanical Engineer's Handbook, John Wiley, New York, 1986.
[25] G.R. Nagpal, Machine Tool Engineering, Khanna Publishers, New Delhi, 1989.